

Phase stability and microstructure of some gel-derived anorthite-based hybrid materials

J. C. DEBSIKDAR*

Idaho National Engineering Laboratory, Idaho Falls, ID 83415, USA

The technical feasibility for producing five different anorthite-based binary and ternary hybrid ceramics containing zirconia and/or silicon carbide whiskers and/or gel-derived *in situ* formed mullite whiskers was examined. The crystallization behaviour of the anorthite and the mullite gels and the phase stability of the hybrid ceramics were studied by X-ray diffractometry. The densification behaviour of the gel-derived materials, including the binary and the ternary composition materials, was examined by measuring densities of the sintered specimens by the immersion method. The microstructures were studied by scanning electron microscopy, supplemented by energy dispersive X-ray spectrometry. The results show the technical feasibility for producing anorthite-based fully dense binary and ternary hybrid ceramics of stable compositions containing zirconia and/or silicon carbide whiskers. However, the compositions containing mullite as a constituent produced hybrid ceramics with *in situ* formed rod-like corundum crystals as the dispersed phase. Discrete monoclinic zirconia was present in all compositions containing this material.

1. Introduction

Anorthite, a calcium aluminosilicate, $\text{CaAl}_2\text{Si}_2\text{O}_8$ (or CAS) is a potentially important glass-ceramic system for producing ceramic composites for thermostructural applications. Glass-ceramic materials are inherently oxidation resistant, fully dense, nominally fully crystalline and, because of their low elastic moduli, lead to good load transfer to the reinforcing fibres in glass-ceramic matrix composites. However, silicon carbide fibre reinforced glass-ceramic matrix composites have shown oxygen embrittlement [1–3]. Oxygen embrittlement in composites is believed to be the consequence of the carbonaceous interface that oxidizes when exposed to air, after the matrices microcrack at the composite elastic limit. Therefore, two approaches are considered important: (1) increasing the composite elastic limit upwards with a class of hybrid ceramic matrix, and (2) creation of mechanically weak, yet oxidatively stable, interface. The first approach is based on the concept that if fracture toughness of the matrix can be increased while maintaining a fairly low elastic modulus, the point of first microcrack can be significantly increased. This has been accomplished in glass-ceramic matrices by SiC whisker reinforcement of the matrix (while still maintaining the primary continuous fibre reinforcement of the composite structure).

A variety of ceramic particulates and whiskers may be used to generate a hybrid-matrix material of improved fracture toughness. The improved fracture toughness of such a hybrid material may be the result of several different mechanisms, such as: by deflection

of the crack in another direction, by crack bridging (i.e. the dispersed phase holding two faces of the hybrid-matrix together) and, by absorption of crack propagation by pullout of the whisker from its original location in the matrix phase. Moreover, if particles of zirconia (ZrO_2) are used as the dispersed phase, a metastable zirconia phase (tetragonal zirconia) may be retained either by temperature and/or pressure and martensitically transforms (into monoclinic zirconia) in the crack-tip stress field and inhibits crack propagation; thereby, increasing the fracture toughness of the material [4–6]. Furthermore, when both ZrO_2 and SiC whiskers are used as dispersed phases, the combination of these multiple toughening mechanisms has been found to result in tougher mullite composite than (1) that achieved by either mechanism by itself, or (2) the sum of the two processes [7]. Other potential advantages of hybridization include the increase in shear and transverse (90°) strengths, increased erosion resistance and, consequently, the material's sensitivity to oxidation embrittlement would be expected to reduce substantially. In other words, controlling the matrix fracture energy by hybridization appears to be an effective way to enhance composite behaviour. However, the thermochemical stability of the dispersed phase(s) and the matrix material is an important issue. In this work, the stability of the phases of anorthite-based hybrid materials containing ZrO_2 , SiC whiskers, as well as a combination of these, was studied. Other compositions studied in this work are based on the recent report [8] that fluorine ion (F^-)-doped mullite ($3\text{Al}_2\text{O}_3 \cdot 2\text{SiO}_2$) gel precursor can

* Present Address: US Department of the Interior, Bureau of Mines, Tuscaloosa Research Center, P.O. Box L, University of Alabama Campus, Tuscaloosa, Al 35486, USA.

be converted into needle-like mullite (mullite whiskers) materials by the appropriate heat-treatment method. Following this work, we decided to examine the technical feasibility of producing anorthite-based hybrid material containing *in situ* formed mullite whisker, and a mixture of mullite whisker and ZrO_2 as the dispersed phases.

For the purpose of this study, a hybrid ceramic is defined as a nominally fully consolidated product, produced by sintering a mixture of ceramic constituents in the desired ratio(s), in which the ceramic constituents retain their compositional identity and phase relationships. This communication presents the preliminary experimental results relating to crystallography and microstructures of anorthite-based binary and ternary hybrid ceramic materials containing zirconia, silicon carbide whiskers, and calcined (fluorine-doped) mullite gel particulates as the dispersed phase(s).

2. Experimental procedure

The compositions of the ceramic hybrid materials studied are given in Table I.

Out of the four ceramic constituents (namely, anorthite, F'-mullite, ZrO_2 and SiCw) used in this work, sol-gel precursors of anorthite (CAS) and 3.5 wt % fluorine-doped mullite (F'-mullite) were synthesized in the laboratory, and ZrO_2 and SiCw were obtained from commercial sources. The commercial sources of these starting materials, as well as those used for synthesizing CAS and F'-mullite gels are listed in Table II.

2.1. Synthesis of anorthite gel

In a round-bottomed reaction flask 435 ml (99% pure) $Si(OC_2H_5)_4$ was diluted with 200 ml $C_3H_7(OH)^i$ and hydrolysed with 25 ml nanopure acidulated water (acidulated with 5 ml 70% conc. HNO_3) for approximately 6 h at 80 °C. 500 g (95% pure) $Al(OC_4H_9)_3$ and 200 ml $C_3H_7(OH)^i$ were added to the hydrolysed $Si(OC_2H_5)_4$ solution at the ambient temperature. The resulting solution was cloudy at first and, subsequently, became clear (yellowish) on addition of 5 ml acetylacetone. The solution was refluxed for 4 h at 80 °C; the volume of the solution reduced by boiling off $C_3H_7(OH)^i$, and then a saturated ethanolic solution of 228 g $Ca(NO_3)_2 \cdot 4 H_2O$ was added to the hot mixed-alkoxide solution. A white gelatinous precipitate formed at first, which dissolved on stirring to produce a turbid solution (or sol). The solution (or sol) was boiled off to reduce the volume before hydrolysing it at the ambient temperature with 300 ml nanopure water to produce a transparent gel in less than 5 min. The gel was dried in an oven at ~ 100 °C for approximately 7 days and then ground in a plastic bottle using alumina balls to produce the anorthite gel powder for characterization.

2.2. Synthesis of fluorine-doped mullite gel

In a round-bottomed reaction flask, 130 ml

TABLE I Composition of ceramic hybrid materials

Sample composition	Sample designation
Anorthite ($CaAl_2Si_2O_8$) + 30 vol % ZrO_2	CAS + ZrO_2
Anorthite ($CaAl_2Si_2O_8$) + 30 vol % silicon carbide whiskers (SiCw)	CAS + SiCw
Anorthite ($CaAl_2Si_2O_8$) + 30 vol % Fluorine-doped (3.5 wt %) Mullite ($3Al_2O_3 \cdot 2SiO_2$)	CAS + F'-mullite
[Anorthite ($CaAl_2Si_2O_8$) + 30 vol % ZrO_2] + 30 vol % silicon carbide whisker (SiCw)	(CAS + ZrO_2) + SiCw
[Anorthite ($CaAl_2Si_2O_8$) + 30 vol % ZrO_2] + 30 vol % Fluorine doped (3.5 wt %) mullite	(CAS + ZrO_2) + F'-mullite

TABLE II Sources of starting materials

Materials	Source
Tetraethoxysilane, $Si(OC_2H_5)_4$	Johnson Matthey Alfa Products, Ward Hill, MA 01835
Aluminium sec-butoxide, $Al(OC_4H_9)_3$	Johnson Matthey Alfa Products, Ward Hill, MA 01835
Calcium nitrate tetrahydrate, $Ca(NO_3)_2 \cdot 4H_2O$	Johnson Matthey Alfa Products, Ward Hill, MA 01835
Isopropanol, $C_3H_7(OH)^i$	Johnson Matthey Alfa Products, Ward Hill, MA 01835
Concentrated hydrofluoric acid, HF	Johnson Matthey Alfa Products, Ward Hill, MA 01835
Ethanol, $C_2H_5(OH)$	Johnson Matthey Alfa Products, Ward Hill, MA 01835
Concentrated nitric acid, HNO_3	Johnson Matthey Alfa Products, Ward Hill, MA 01835
Zirconia, ZrO_2	Fisher Scientific, Fair Lawn, NJ 07410
Silicon carbide whisker, SiCw (Huber XPW2 experimental SiCw)	J. M. Huber Corp., Borger, TX 79008

$Si(OC_2H_5)_4$ was diluted with an equal volume of anhydrous ethanol and hydrolysed for 6 h at 60 °C with 50 ml nanopure water acidified with 3 ml conc. HNO_3 . Separately, 450 ml (95% pure) $Al(OC_4H_9)_3$ was hydrolysed at 90 °C in 2 l nanopure water to produce a slurry of aluminium hydrous oxide. The slurry was peptized at the same temperature using 10 ml conc. HNO_3 to produce a clear boehmite sol. The boehmite sol was cooled to the room temperature before mixing with the hydrolysed $Si(OC_2H_5)_4$ or the silica sol. To the mixed sol, 9 ml commercial 49% HF was added under constant stirring.

Initially, some precipitate was formed. The precipitate dissolved after a short while, followed by gelation in less than 15 min to produce a transparent

gel. The gel was dried in an oven at $\sim 100^\circ\text{C}$ for approximately 7 days and then ground in a plastic bottle using alumina balls to produce the F'-mullite gel powder for characterization.

2.3. Characterization of gels

Both anorthite and F'-mullite gels were characterized by differential thermal (DTA) and X-ray powder diffraction analyses methods to examine their crystallization behaviour. For DTA, the samples were heated at $10^\circ\text{C min}^{-1}$ in a free-flowing air environment using an Omnic Therm Thermal Analysis Module 1500 interfaced with computerized system for data analysis and recording. Philips PW 1729 automated diffractometer was used for X-ray diffraction. For X-ray powder diffraction analysis, the gel samples after heat treatment at different temperatures were scanned from $2\theta = 10^\circ\text{--}70^\circ$ at 1°C min^{-1} using monochromatic CuK_α radiation with a nickel filter.

2.4. Production of hybrid ceramics

Anorthite (CAS) gel, heated to 1100°C , was wet-milled in acetone in a plastic bottle using alumina balls and then dried in an air oven at $\sim 100^\circ\text{C}$ to produce the starting powder for fabricating CAS, CAS + ZrO_2 , CAS + SiCw, CAS + F'-mullite, CAS + ZrO_2 + SiCw and CAS + ZrO_2 + F'-mullite ceramics. ZrO_2 powder was used as-received. The as-received SiCw was washed with aqueous HF to remove leachable impurities and then fractionated to remove large agglomerates, followed by acetone wash and drying. The morphology of the SiCw after washing and fractionation is shown in Fig. 1. F'-mullite gel

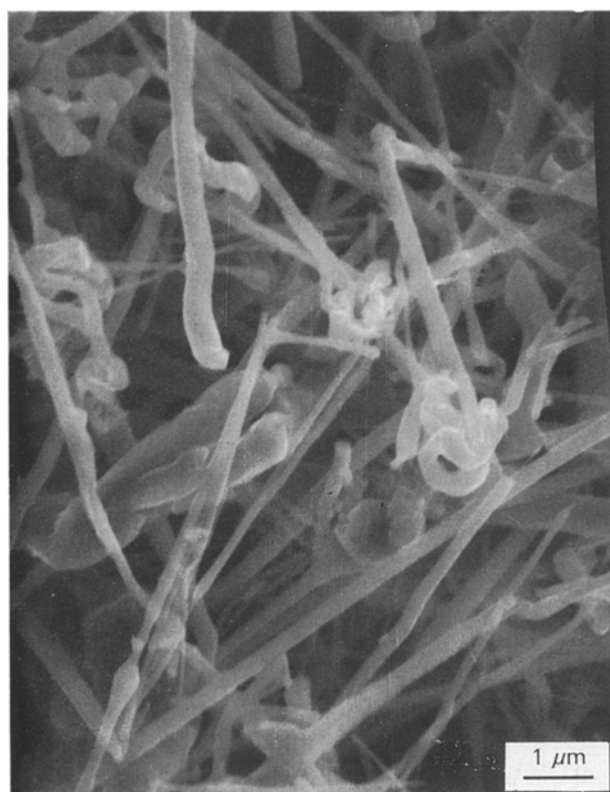


Figure 1 Morphology of silicon carbide whiskers.

was precalcined at 650°C for 2 h in a Lindbergh furnace, ground in a plastic bottle using alumina balls, and then screened through a $150\ \mu\text{m}$ screen. The ($-$) $150\ \mu\text{m}$ fraction of the F'-mullite powder was used to fabricate F'-mullite ceramic. This powder was also used as the mullite constituent for producing ceramics hybrids.

Ceramic hybrid formulations (Table I) containing the desired proportions of the constituents were wet-mixed in acetone in plastic bottles using alumina balls. The slurries thus produced were oven-dried at $\sim 70^\circ\text{C}$. The dried mixes were pelletized by uniaxial pressure at $\sim 69\ \text{MPa}$ and, subsequently, these pellets were pressed further at $\sim 206\ \text{MPa}$ by cold isostatic pressing. Pellets of CAS and F'-mullite were fabricated by the same procedure for evaluation of the hybrid ceramic compositions containing these materials. The pellets were sintered at 1450° and 1550°C in an Astro furnace in free-flowing nitrogen atmosphere. A graphite sample holder with four groves was used for sintering the "green" pellets. On pellet each of four compositions was placed in each groove with a layer of a mixture of boron nitride and silicon carbide powders on all sides to avoid direct contact of the samples with the graphite walls. The sintering schedule consisted of $10^\circ\text{C min}^{-1}$ heating rate, a 2 h at the sintering temperature, and natural cooling of the furnace by turning off the power. Some samples containing F'-mullite were sintered at 1300°C using the same heating, holding and cooling schedules.

The densities of the sintered pellets were determined (by immersion method) to examine the densification of CAS, F'-mullite, and the CAS-based hybrid compositions listed in Table I. The phase compositions of the sintered pellets were studied by X-ray powder diffraction method. The microstructures of the sintered products were examined on polished ($1\ \mu\text{m}$ finish), gold-coated surfaces with an AMRAY 1830 scanning electron microscope (SEM). Moreover, energy dispersive X-ray analysis capability of the SEM was utilised to examine the compositional change(s) of a few specimens.

3. Results and discussion

3.1. Characterization of gel

The DTA curves of anorthite (Fig. 2) and F'-mullite (Fig. 3) both showed exothermic peaks around 400°C due to oxidative removal of volatiles, and crystallization peaks at 1050° and a little over 1250°C , respectively. The DTA curve of the anorthite gel did not show separate peaks representing the loss of residual organics and thermochemical reactions involving decomposition of calcium nitrate and the removal of nitrate ions. However, considering the synthesis chemistry of the anorthite gel, the amount of residual organics in this gel would be very small. Furthermore, the X-ray data on this gel (shown later) did not indicate any crystallization phenomenon occurring up to 600°C or more. Therefore, the broad low-temperature exothermic peak of the anorthite gel is probably related mainly to the removal of the nitrate ions from the gel. Moreover, the absence of any further thermal change prior to the crystallization exotherm at $\sim 1050^\circ\text{C}$

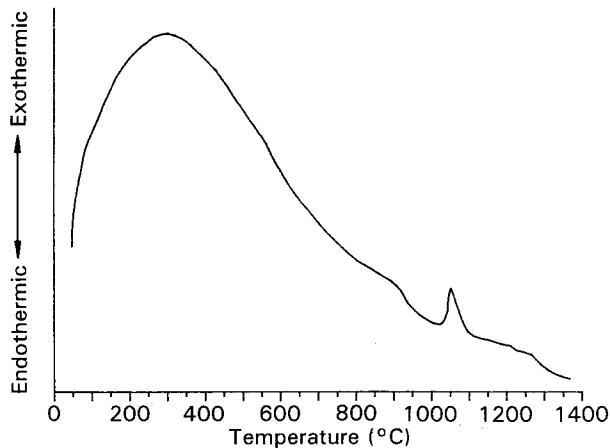


Figure 2 DTA curve of anorthite gel.

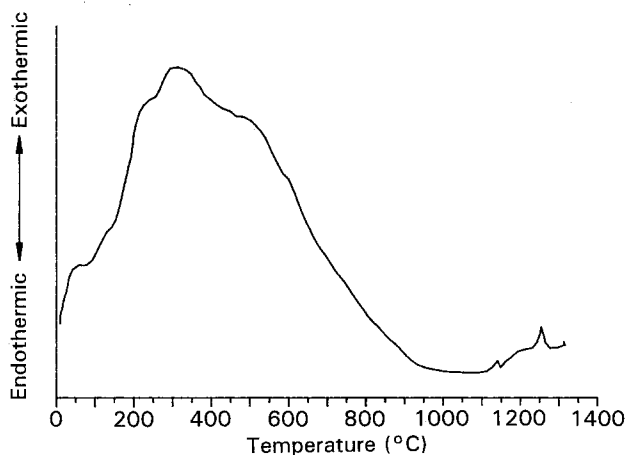


Figure 3 DTA curve of F'-mullite gel.

suggests that the conversion of the gel to anorthite takes place without the formation of any intermediate crystalline phase.

F'-mullite gel showed overlapping exothermic peaks at the lower temperatures. The thermal changes in the temperatures range up to approximately 450 °C was associated with more than 95 % total weight loss (not shown) which must be related to the loss of residual organics as well as the loss resulting from the reaction of hydrofluoric acid with the gel to form volatile fluorosilic acid. However, the X-ray data on this gel suggest that the exothermic behaviour of the gel beyond 500 °C could be related to the nucleation and crystallization of η -Al₂O₃. A small weight loss (less than 5 %) in this temperature range is probably due to the continuous loss of the fluorinated product and residual organics, if any.

The X-ray diffractograms showing the crystallization behaviour of anorthite and F'-mullite gels are shown in Figs 4 and 5, respectively. These results show that anorthite and F'-mullite gels can be nominally fully crystallized at 1100° and 1250 °C, respectively, which are consistent with the DTA results. However, both the X-ray and the DTA data suggest that, while the anorthite gel crystallized directly to produce anorthite ceramic, the mullite gel initially crystallized to η -Al₂O₃ and amorphous SiO₂ which subsequently reacts to produce mullite crystals at ~ 1250 °C or less.

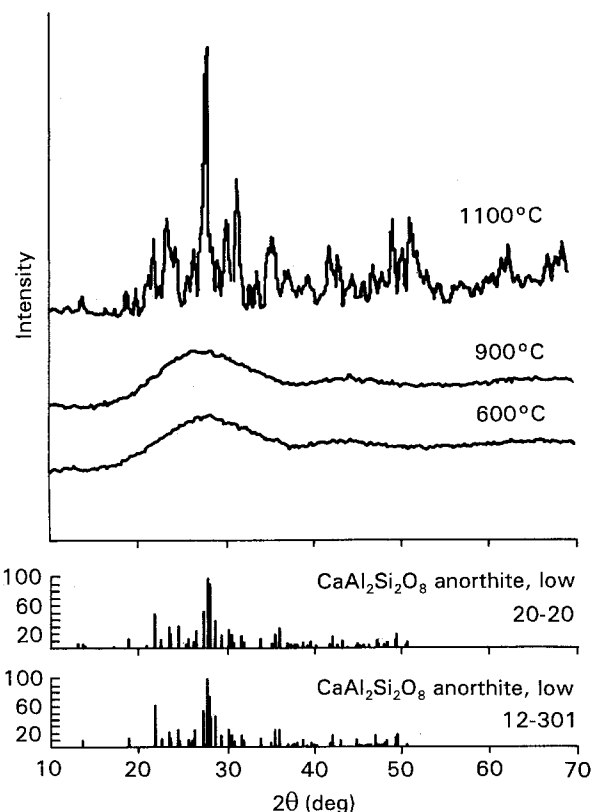


Figure 4 Crystallization behaviour of anorthite gel.

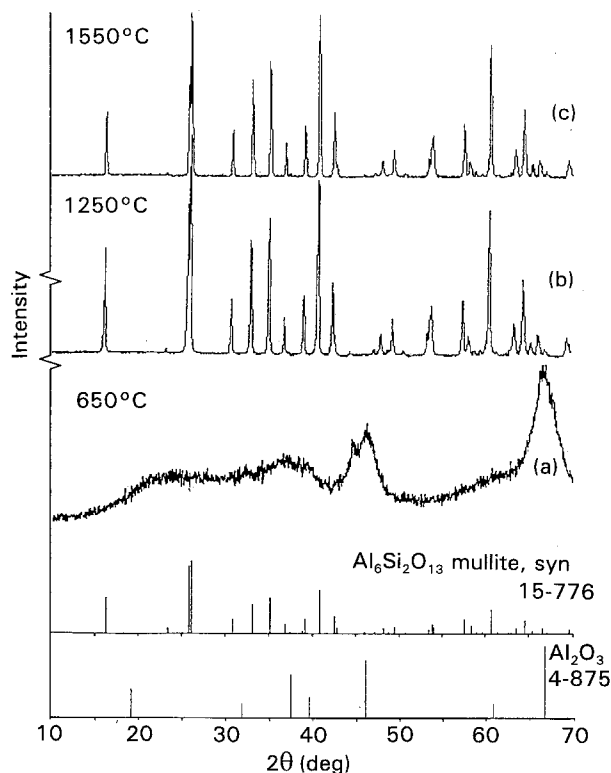


Figure 5 Crystallization behaviour of F'-mullite gel.

3.2. Production of hybrid ceramics

For the purpose of this study, a hybrid ceramic is defined as a nominally fully consolidated product, produced by sintering a mixture of ceramic constituents in the desired ratio(s), in which the ceramic constituents retain their compositional identity and phase relationships. Therefore, in the present study,

the densification behaviours of the hybrid compositions were examined first, before studying the phase compatibility and the microstructures of those hybrid ceramics.

The sintered densities of hybrid ceramic pellets sintered at 1450° and 1550 °C are shown in Table III. The density data indicate that sintering at 1450 °C is not adequate to produce dense hybrid ceramics of the studied compositions, and that a sintering temperature around 1500 °C is required to produce high-density hybrid ceramics from these compositions. It must be mentioned here that almost all the 1550 °C sintered samples exhibited defects in the form of close porosity and/or cracks and, consequently, systematic sintering studies are required to produce fully dense defect-free hybrid ceramics of the above compositions which is beyond the scope of the present investigation. In the present work, it was decided to study the phase compositions and microstructures on the samples sintered at 1550 °C. Moreover, hybrid compositions containing F'-mullite were also sintered at 1300 °C to examine the nature of chemical interactions between the constituents at this temperature.

3.3. Phase composition

The X-ray diffractograms of CAS (Fig. 6) and F'-mullite (Fig. 5c) show that these materials are chemically stable at 1550 °C. The phase stability of the constituents in hybrid compositions, CAS + ZrO₂ and (CAS + ZrO₂) + SiCw, remained unchanged at 1550 °C sintering temperature as shown in X-ray diffractograms of Figs 7 and 8, respectively. Because the composition (CAS + ZrO₂) + SiCw was stable at 1550 °C (Fig. 8), it was presumed that CAS + SiCw would also remain stable at 1550 °C and, as such, X-ray analysis of this composition was not performed. In all compositions containing ZrO₂, however, the sintered hybrid ceramic products showed the presence of monoclinic polymorph only (Figs 7 and 8). It may be mentioned here that even though these ZrO₂-containing samples were sintered in the tetragonal-ZrO₂ phase field, the sintered products did not retain the tetragonal phase metastably. This may be related to the large grain sizes of ZrO₂ in the sintered products.

The phase compositions of CAS + F'-mullite as a function of three different sintering temperatures (e.g.

TABLE III Densities of CAS, F'-mullite and hybrid ceramics as a function of sintering temperature

Composition	Sintered Density (g cm ⁻³) at	
	1450 °C	1550 °C
CAS	1.8	2.7
F'-mullite	1.4	2.8
CAS + ZrO ₂	3.4	3.6
CAS + SiCw	1.8	2.9
CAS + F'-mullite	2.3	2.6
(CAS + ZrO ₂) + SiCw	2.7	3.3
(CAS + ZrO ₂) + F'-mullite	3.5	3.6

1300, 1450, and 1550 °C) are shown in Fig. 9. The diffraction pattern of the 1300 °C sintered material corresponded to a mixture of CAS and mullite. No additional peak was observed. However, when the

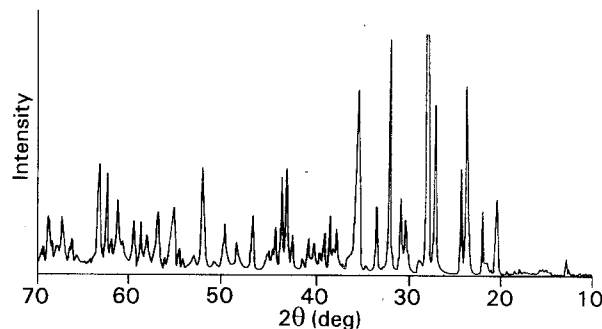


Figure 6 X-ray diffractogram of 1550 °C sintered gel-derived CAS.

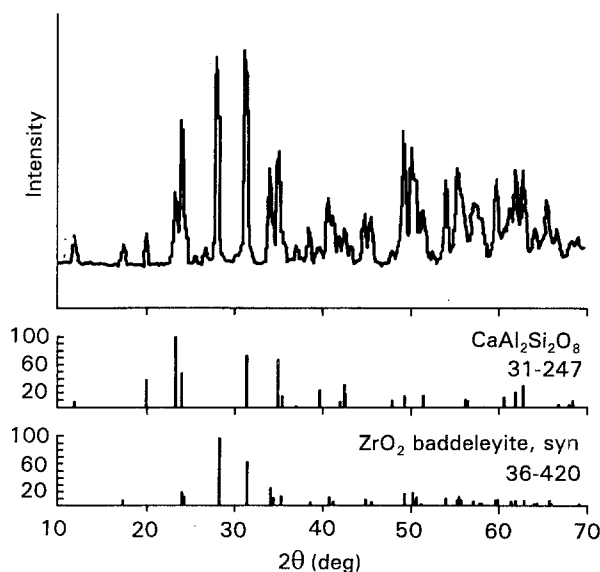


Figure 7 X-ray diffractogram of 1550 °C sintered CAS + ZrO₂ hybrid ceramic.

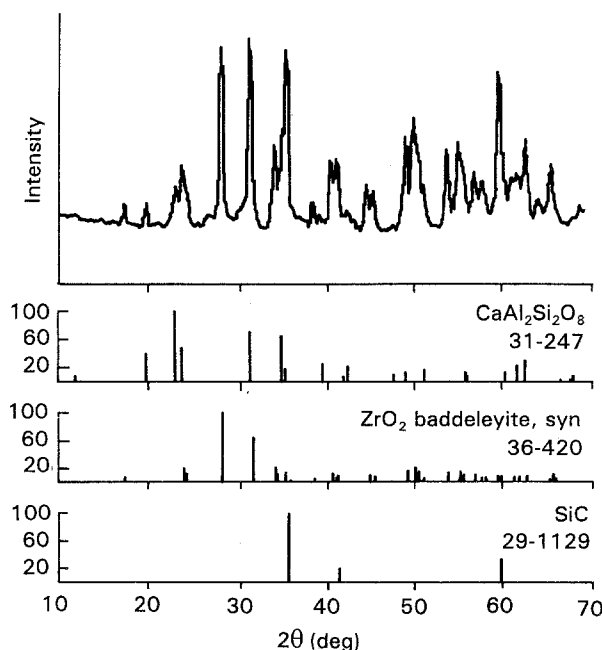


Figure 8 X-ray diffractogram of 1550 °C sintered (CAS + ZrO₂) + SiCw hybrid ceramic.

composition was sintered at 1450 °C, the sintered material contained CAS, mullite and, in addition, a small amount of sillimanite ($\text{Al}_2\text{O}_3 \cdot \text{SiO}_2$ or Al_2SiO_5) and corundum (Al_2O_3), as shown in Fig. 9b. At 1550 °C sintering temperature, the phases corresponding to only CAS and corundum were indicated. Sillimanite which was formed at 1450 °C, was not present in the 1550 °C sintered material. Based on these observations and also the fact that mullite, by itself, was stable up to 1550 °C (Fig. 5c), it would appear that the progressive decomposition of mullite phase in CAS + F'-mullite mixture was due to its chemical reactions with CAS, the amount depending on the relative proportion of F'-mullite in the CAS + F'-mullite composition. The nature of chemical interactions between CAS and F'-mullite was also similar in CAS + ZrO_2 + F'-mullite as can be seen in Fig. 10. However, further research is necessary to understand fully the exact nature and sequence of the chemical reactions. It may be pointed out here that ZrO_2 retained its identity in the 1550 °C sintered (CAS + ZrO_2) + F'-mullite mixture (Fig. 10) as a monoclinic polymorph. To verify the chemical compatibility of the hybrid composition F'-mullite + 30 vol % ZrO_2 , a sample of this composition was sintered separately at 1550 °C. The X-ray diffractogram of this sample showed a phase assemblage consisting of F'-mullite and monoclinic ZrO_2 (Fig. 11). In summary, the X-ray data on the products of 1550 °C sintered hybrid compositions show that all the studied compositions, except those which contained both CAS + F'-mullite, can potentially form fully dense hybrid ceramics.

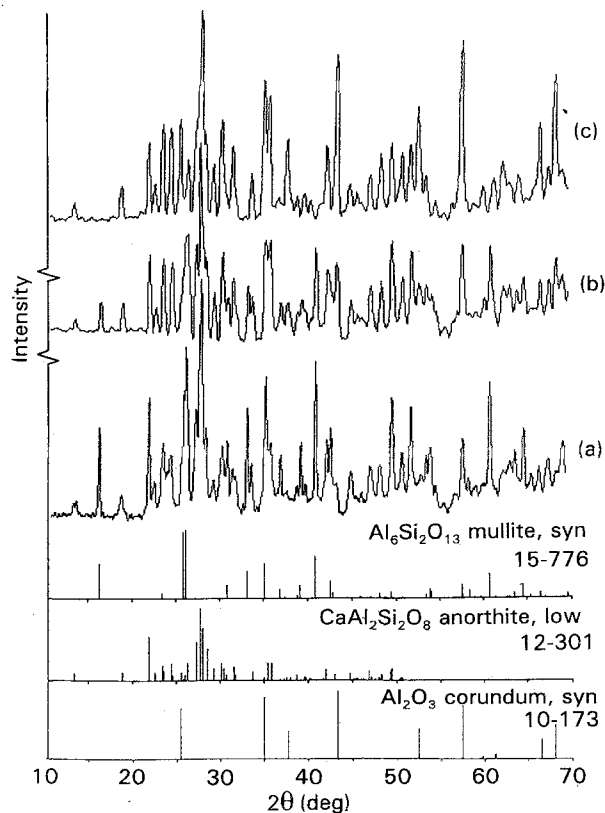


Figure 9 X-ray diffractograms of CAS + F'-mullite as a function of sintering temperatures. (a) 1300 °C, (b) 1450 °C, and (c) 1550 °C.

3.4. Microstructure

A scanning electron micrograph of 1550 °C sintered CAS gel is shown in Fig. 12. The microstructure of the material appears to be (glass-like) featureless even though the X-ray diffractogram (Fig. 6) shows that the material is nominally fully crystalline. The apparent featureless nature of the sintered CAS microstructure may be due to the fact that the size of the crystallites is not large enough to be resolved at this magnification. The microstructure of the 1550 °C sintered F'-mullite showed needle- or rod-like microstructure (Fig. 13) which is consistent with the results reported by Ismail *et al.* [8]. The microstructure of (CAS + ZrO_2) is

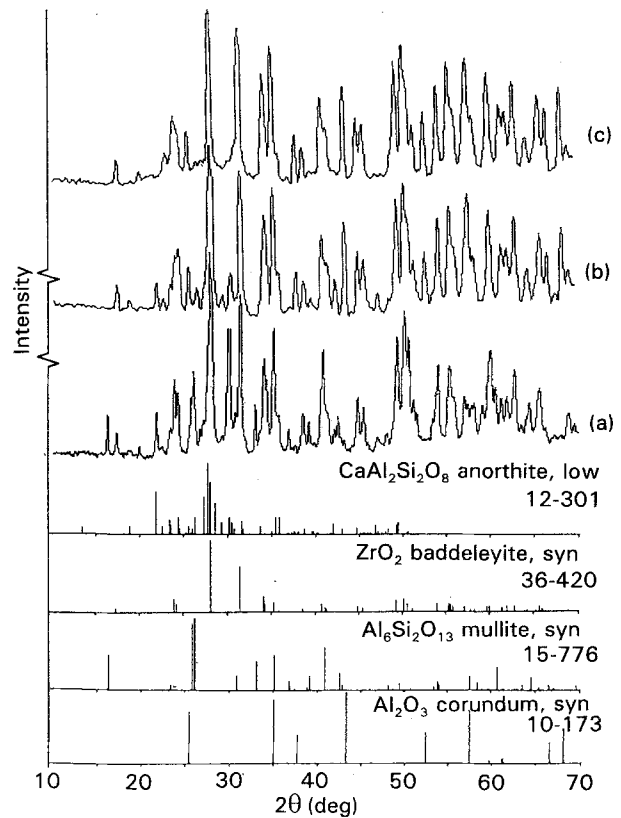


Figure 10 X-ray diffractograms of (CAS + ZrO_2) + F'-mullite as a function of sintering temperature. (a) 1300 °C, (b) 1450 °C, and (c) 1550 °C.

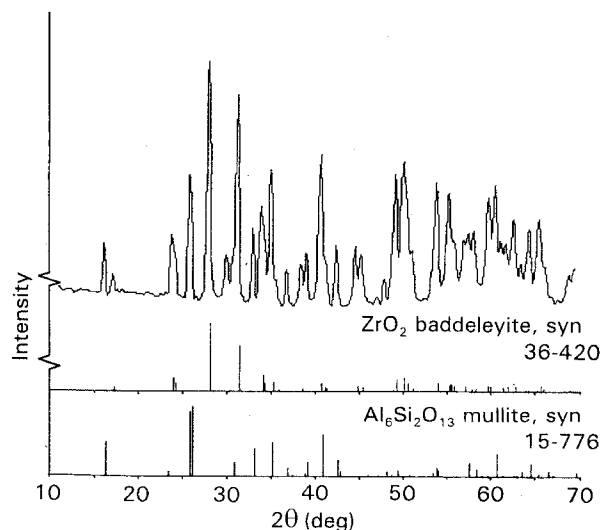


Figure 11 X-ray diffractogram of 1550 °C sintered F'-mullite + ZrO_2 hybrid ceramic.

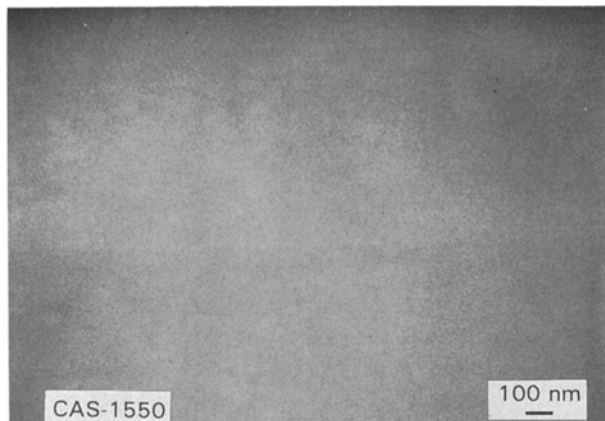


Figure 12 Scanning electron micrograph of 1550 °C sintered gel-derived CAS.

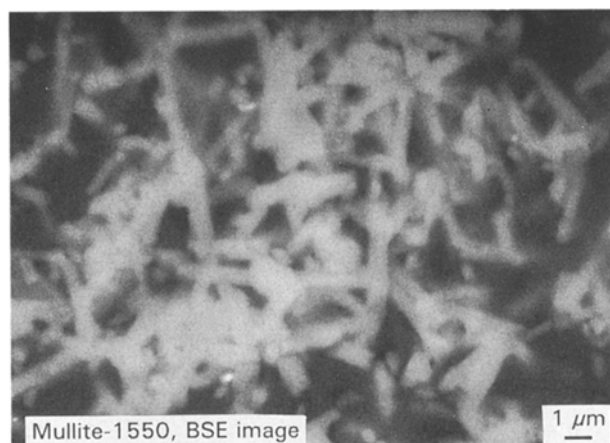


Figure 13 Scanning electron micrograph of 1550 °C sintered gel-derived F'-Mullite.



Figure 14 Scanning electron micrograph of 1550 °C sintered (CAS + ZrO₂) hybrid ceramic.

shown in Fig. 14. The distribution of ZrO₂ phase in this material was non-uniform, the area on top of the micrograph represents the top surface of the pellet during the sintering process. We speculate that during the viscous sintering process, the dispersed ZrO₂ particles tended to settle by gravity leading to non-uniformity of the microstructure. Moreover, a large amount of porosity (most of which is adjacent to the ZrO₂ particles) is present. These results seem to suggest that a sintering schedule involving a somewhat lower sintering temperature and longer holding might be beneficial in producing fully dense (CAS + ZrO₂) hybrid ceramics of uniform microstructure. The microstructure of (CAS + SiCw) (Fig. 15) was highly uniform. Because the needle- or rod-like SiCw dispersed phase formed a network microstructure, and also, because the densities of CAS (2.8 gcm⁻³) and SiCw (~ 3.0 gcm⁻³) are similar, the viscous sintering process did not lead to any significant non-uniformity of distribution of SiCw. Consequently, the microstructure was uniform. EDX analysis was done on this material as well as on the (CAS + ZrO₂) + SiCw material to obtain independent information regarding the existence of discrete SiCw phase indicated in the X-ray diffractogram (Fig. 8) for the (CAS + ZrO₂) + SiCw system. This could not be accomplished due to practical problems of focusing the beam on discrete silicon carbide whiskers. Consequently, the EDX spectrum of the (CAS + SiCw) hybrid material showed a significantly reduced Al/Si ratio (Fig. 16) compared to that of the CAS itself (Fig. 17). However, it was possible to confirm independently the existence of discrete ZrO₂ phase in the (CAS + ZrO₂) + SiCw hybrid material (Fig. 18) as indicated in both the X-ray diffractogram (Fig. 8) as well as the scanning electron micrograph (Fig. 19) of its microstructure.

The microstructures of two compositions containing F'-mullite, namely, (CAS + F'-mullite) and (CAS + ZrO₂) + F'-mullite are shown in Figs 20 and 21, respectively. The microstructures of these materials were uniform. The EDX spectrum of the rod-like phase in (CAS + F'-mullite) composition showed the material to be alumina (Fig. 22) and dispersed in a matrix phase with an Si/Al ratio greater (Fig. 23) than CAS itself (Fig. 17) due to progressive silica enrichment of the CAS matrix (during the sintering

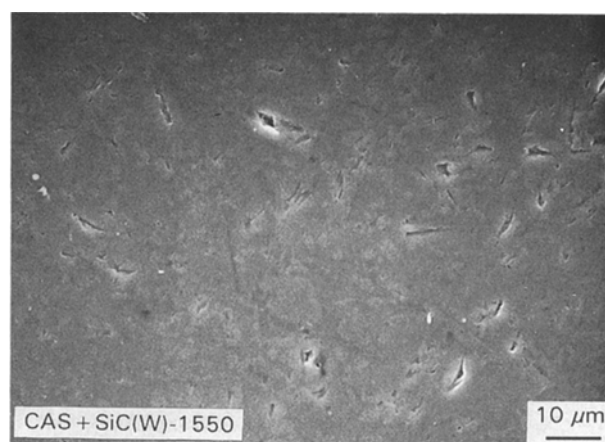


Figure 15 Scanning electron micrograph of 1550 °C sintered (CAS + SiCw) hybrid ceramic.

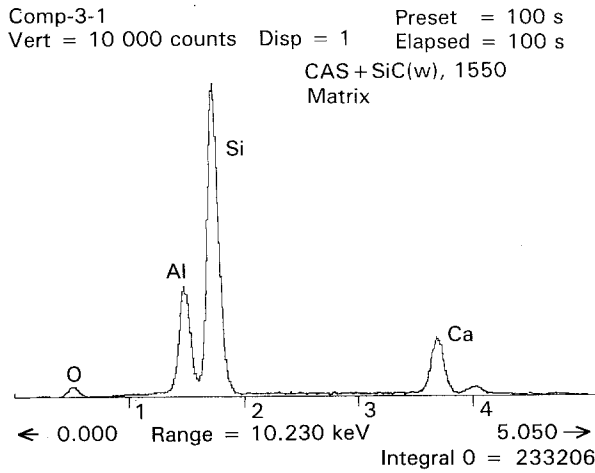


Figure 16 EDX spectrum of 1550°C sintered (CAS + SiCw) hybrid ceramic.

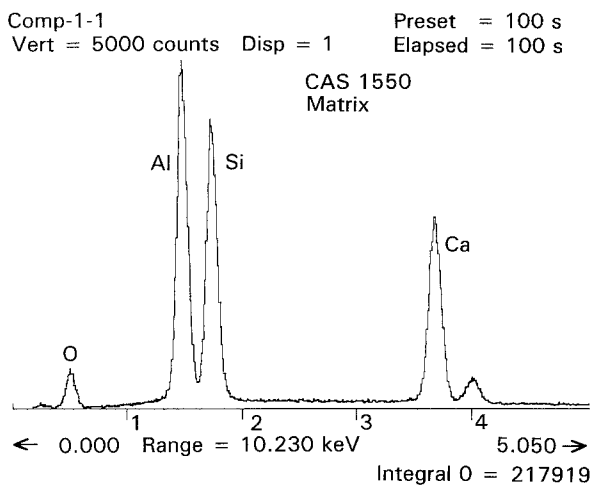


Figure 17 EDX spectrum of 1550°C sintered (CAS + ZrO₂) + SiCw hybrid ceramic.

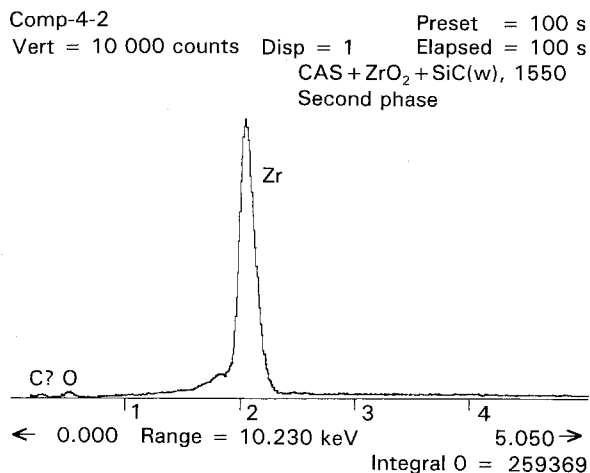


Figure 18 EDX spectrum of ZrO₂ in 1550°C sintered (CAS + ZrO₂) + SiCw hybrid ceramic.

process) resulting from the decomposition of mullite, as discussed in the preceding section. EDX spectra of the rod-like and the matrix phases of the (CAS + ZrO₂) + F'-mullite material were, as expected, almost identical to those shown in Figs 22 and 23, respectively. It is interesting to note that rod-like

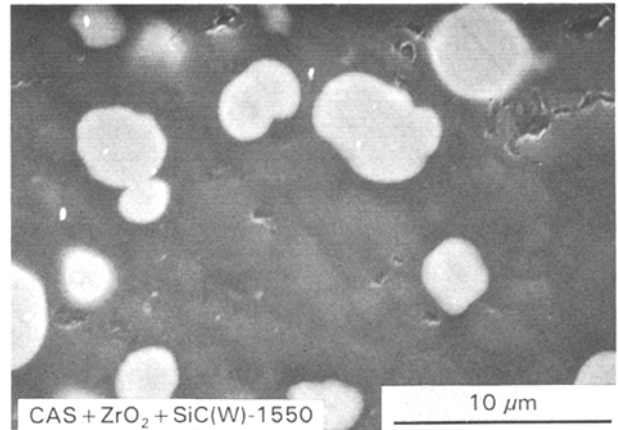


Figure 19 Scanning electron micrograph of 1550°C sintered (CAS + ZrO₂) + SiCw hybrid ceramic.

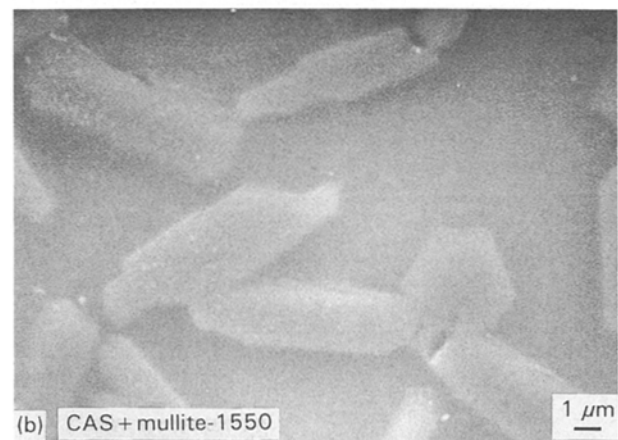
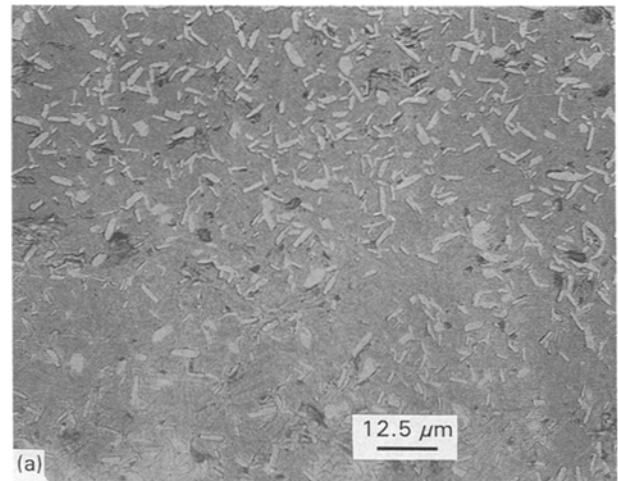


Figure 20 Scanning electron micrographs of 1550°C sintered (CAS + F'-mullite) hybrid ceramic.

(faceted) alumina crystals could be formed *in situ* in some selected compositions containing gel-derived precalcined mullite particulates. It is hypothesized that during the sintering process, F'-mullite gel particulates are converted into the rod-like morphology, and that during subsequent decomposition of mullite, the morphology [8] of the precipitated phase tends to retain the morphology of the parent material. The probable nature of the chemical reactions (see previous section) seems to suggest that such an approach

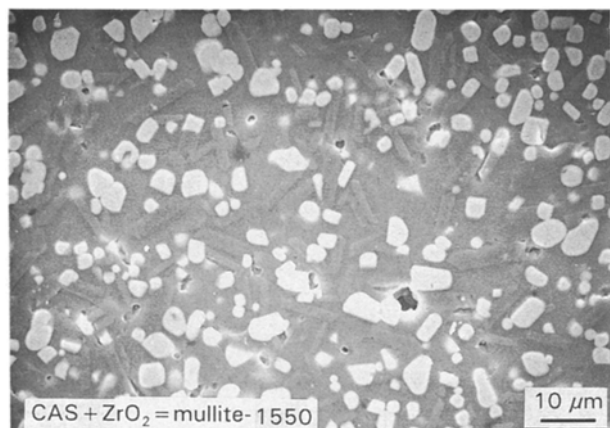


Figure 21 Scanning electron micrograph of 1550°C sintered (CAS + ZrO₂) + F'-mullite hybrid ceramic.

Comp-5-5
 Vert = 20 000 counts Disp = 1 Preset = 100 s
 Elapsed = 100 s
 CAS + mullite, 1550
 Rod-like grain

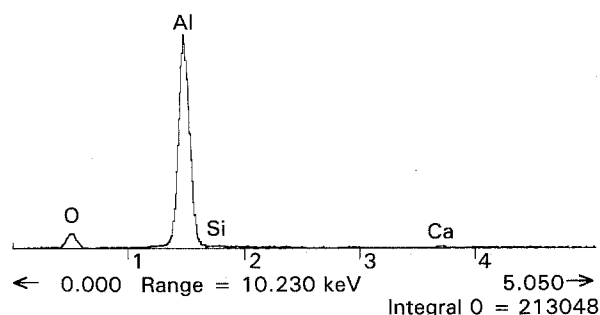


Figure 22 EDX Spectrum of rod-like phase in 1550°C sintered (CAS + F'-mullite) hybrid ceramic.

Comp-5-4
 Vert = 10 000 counts Disp = 1 Preset = 100 s
 Elapsed = 100 s
 CAS + mullite, 1550
 Matrix

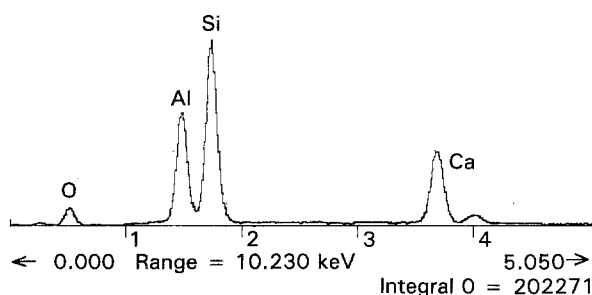


Figure 23 EDX spectrum of the matrix phase of 1550°C sintered (CAS + F'-mullite) hybrid ceramic.

could lead to the development of processes for producing glass-ceramic matrix composites in which the dispersed phase(s) is (are) formed *in situ*. Furthermore, the EDX spectrum (Fig. 24) of the bright particulate phase (Fig. 21) provided evidence (in addition to XRD in Fig. 10) that ZrO₂ could exist as a discrete phase in those hybrid ceramic composites.

Comp-6-3
 Vert = 10 000 counts Disp = 1 Preset = 100 s
 Elapsed = 100 s
 CAS + ZrO₂ + mullite, 1550
 Bright phase

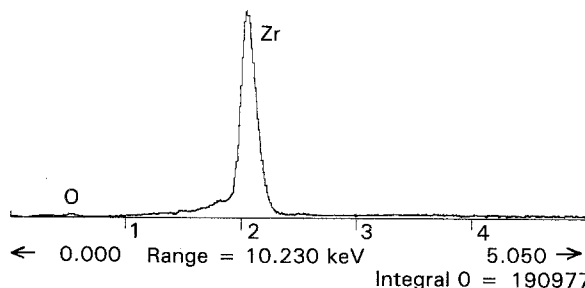


Figure 24 EDX spectrum of the bright particulate phase (Fig. 21) in 1550°C sintered (CAS + ZrO₂) + F'-mullite hybrid ceramic.

4. Conclusions

1. Anorthite, CaAl₂Si₂O₈ (CAS) and 3.5 wt % fluorine-doped mullite, Al₆Si₂O₁₃ (F'-mullite) gels were synthesized, and their crystallization and sintering behaviours were characterized.
2. The gel-derived CAS and F'-mullite materials were mixed with commercial zirconia (ZrO₂) and silicon carbide whiskers (SiCw) to produce the following binary and ternary hybrid ceramics.

CAS + 30 vol % ZrO₂, CAS + 30 vol % SiCw

CAS + 30 vol % F'-mullite

(CAS + 30 vol % ZrO₂) + 30 vol % SiCw

(CAS + 30 vol % ZrO₂) + 30 vol % F'-mullite

3. The result of this study showed that it should be technically feasible to produce fully dense hybrid ceramics of the compositions CAS + 30 vol % ZrO₂, CAS + 30 vol % SiCw and (CAS + vol % ZrO₂) + 30 vol % SiCw (by appropriate sintering schedules) in which the constituents retain their identities.

4. Hybrid ceramics produced from compositions containing both CAS and F'-mullite were all characterized by the formation of rod-like faceted alumina (corundum) phase, resulting from the decomposition of F'-mullite. This approach could have potential applicability for producing glass-ceramic composites in which rod-like corundum crystals are formed *in situ*.

5. ZrO₂ was found to be present as discrete monoclinic phase in all hybrid ceramics in which ZrO₂ was used as a constituent.

Acknowledgements

The experimental work was performed at the Idaho National Engineering Laboratory (INEL) under DOE Contract DE-AC07-761D01570. The author gratefully acknowledges the assistance of A. W. Erickson, S. T. Schuetz, and D. V. Miley, INEL, for X-ray diffractograms, DTA and the scanning electron micrographs. Jim Shirley and Sandra Bodle, US Bureau of Mines, Tuscaloosa Research Center, provided assistance in preparing the manuscript.

References

1. K. M. PREWO and G. K. LAYDEN, "Advanced Fabrication and Characterization of SiC Fiber Reinforced Glass-Ceramic Matrix Composites", UTRC Report R84-916175-1 on ONR Contract N00014-81-C-0571 (1984).
2. K. M. PREWO, J. J. BRENNAN and G. K. LAYDEN, *Am. Ceram. Soc. Bull.* **65** (1986) 305.
3. J. F. MANDELL, K. C. C. HONG and D. M. GRANDE, *Ceram. Eng. Sci. Proc.* **8** (1987) 937.
4. R. M. McMEEKING and A. G. EVANS, *J. Am. Ceram. Soc.* **65** (1982) 242.
5. S. BLOCK, G. J. PIERMARINI, B. J. HOCKEY, B. R. LAWN and R. G. MUNRO, *ibid.* **69** (1986) C-125.
6. A. H. HENER, *ibid.* **70** (1987) 689.
7. P. F. BECKER and T. N. TIEGS, *ibid.* **70** (1987) 651.
8. MAHAMED G. M. U. ISMAIL, HIROSHI ARAI, ZENZIRO NAKAI and TAKUJI AKIBA, *ibid.* **73** (1990) 2736.

*Received 3 August 1992
and accepted 31 August 1993*